Lawsonite-type phase transitions in hennomartinite, $SrMn_2[Si_2O_7](OH)_2 \cdot H_2O$

Eugen Libowitzky and Thomas Armbruster

Laboratorium für chemische und mineralogische Kristallographie der Universität Bern, Freiestrasse 3, CH-3012 Bern, Switzerland

Abstract

Phase transitions similar to those observed at low temperatures in lawsonite, $CaAl_2[Si_2O_7](OH)_2 \cdot H_2O$, were recorded at ~95 and ~150 °C in hennomartinite, $SrMn_2[Si_2O_7](OH)_2 \cdot H_2O$. The room temperature structure of the natural phase was refined from X-ray single-crystal data in space group $P2_1cn$ and that of the >150 °C phase at 245 °C in space group $Cmcm$. The structures are isotypic to the low-temperature and room temperature structures of lawsonite. The $P2_1cn$ structure of hennomartinite exhibits twinning parallel to (100) with additional disorder mainly involving the H positions. As indicated by a split O position (O5), disorder and twinning must also be considered in the $Cmcm$ structure. Similar to lawsonite, the driving force of the phase transitions is apparently the development of cooperative hydrogen bonds. At low temperatures the H atoms shift toward neighboring O atoms forming strong hydrogen bonds.

The transition temperatures were determined by monitoring the intensities of critical reflections over the temperature range from −163 to 245 °C. The low-temperature boundary of the $Cmcm$ phase is characterized by the appearance of the 017 reflection (among other C-centering forbidden reflections) below 150(5) °C. The high-temperature boundary of the twinned room temperature phase is characterized by a dramatic enhancement of the intensity of the 406 reflection below 95(5) °C. Between 95 and 150 °C (in analogy to lawsonite) the average space group $Pmcn$ is proposed, which is the mediating sub-super group between $P2_1cn$ and $Cmcm$.

After one heating and cooling cycle, splitting of $hk0$ reflections (observed in ω scans) below ~100 °C indicates that the true, relaxed room temperature structure represents a monoclinic derivative of the natural, initially determined $P2_1cn$ average structure. Moreover, a decrease of the a unit-cell parameter and the unit-cell volume during the 245 °C data collection suggests a temperature-controlled structural evolution of hennomartinite from disorder and small twin domains in the natural phase to large twin domains caused by annealing at elevated temperatures.

Introduction

Only recently, hennomartinite, $SrMn_2[Si_2O_7](OH)_2 \cdot H_2O$, was described as a new mineral from the Wessels Mine of the Kalahari manganese ore fields (Armbruster et al. 1993). It occurs as tiny brown crystals in small veins crosscutting almost pure sugilite + serandite-pectolite. The orthorhombic unit-cell parameters were refined to $a = 6.255(1)$, $b = 9.034(2)$, $c = 13.397(2)$ Å, $Z = 4$. The structure was determined by Armbruster et al. (1992) to be of the lawsonite type, $CaAl_2[Si_2O_7](OH)_2 \cdot H_2O$, space group $Cmcm$ (Baur 1978), where Ca is replaced by Sr, and Al by Mn^{3+}. The MnO_6 octahedra, which form edge-sharing chains parallel to a (interconnected by Si_2O_7 groups), exhibit a Jahn-Teller distortion with four short and two long Mn^{3+}-O distances. However, X-ray single-crystal data could only be refined to a final $R = 4.8\%$, and the positions of the H atoms could not be located because of the heavy atoms in the structure and the disorder of the H_2O molecules.

The present investigation was initiated by recent observations of reversible, low-temperature phase transitions in lawsonite (Libowitzky and Armbruster 1995). The authors showed that below 0 °C the $Cmcm$ structure of lawsonite changes to $Pmcn$. Below approximately −120 °C the symmetry is further reduced to space group $P2_1cn$. Both transitions are mainly characterized by successive loss of mirror planes owing to rotations of the OH groups and the H_2O molecules, whereas the rigid aluminosilicate framework remains almost unchanged.

Because hennomartinite is isotypic to lawsonite, it was interesting to investigate whether it shows similar phase transitions. However, because of the expanded framework dimensions, transition temperatures above those in lawsonite were expected. It also seemed important to localize the H-atom positions to facilitate comparison between probable transition phases in hennomartinite and those in lawsonite.

Experimental procedure and X-ray data collection

Hennomartinite crystals from the same hand specimen of a sugilite-rich rock as described by Armbruster et al.

TABLE 1. Experimental parameters of the hennomartinite refinements at 22 and 245 °C

T (°C)	22	245
Space group	$P2_1cn$*	$Cmcm$
a (Å)	6.247(1)	6.255(1)**
b (Å)	9.034(1)	9.067(1)
c (Å)	13.401(2)	13.431(2)
N_{refl}	3711	3973
N_{unique}	2813	1271
N_{param}	111	51
R_{int} (%)	4.4†	1.8
R (%)‡	2.0	2.3
R_w (%)‡	3.8†	2.6
Gof‡	1.19†	1.34
Resid. (e⁻/Å³)	<0.6	<1.0

* Shift in origin of (0,¼,0).
** Decreasing from 6.260 to 6.249 Å during the 245 °C measurement.
† Refined with SHELXL93; consequently F^2 instead of F is used. $R = \Sigma|F_{obs}| - |F_{calc}|/\Sigma|F_{obs}|$, $R_w = [\Sigma w(|F_{obs}| - |F_{calc}|)^2/\Sigma w|F_{obs}|^2]^{1/2}$, and $Gof = [\Sigma w(|F_{obs}| - |F_{calc}|)^2/(N_{refl} - N_{param})]^{1/2}$.
‡ For $F_{obs} > 6\sigma_{Fobs}$.

(1992, 1993) were used for the present investigation. An electron microprobe analysis of hennomartinite that corresponds to a nearly end-member composition is given by Armbruster et al. (1992, 1993). In a preliminary investigation, fragments of hand-picked crystals were checked by the X-ray precession method (Mo$K\alpha$ radiation) for twinning, systematic absences, and general sample quality. Most crystals were rejected because of slight peak splitting or smearing recorded on films or because of a general lack of sufficient diffractive intensity in the very small crystal fragments. Some of the most promising crystals were rejected even after analysis on the single-crystal diffractometer because of uneven backgrounds, split or smeared reflections (in ω), or generally weak intensities. Extremely flat or broad reflections in θ (indicating a glassy state) were not observed.

An ellipsoid-shaped fragment of hennomartinite (the best crystal of the preliminary test procedure), 0.13 × 0.17 × 0.22 mm in size, was mounted on a silica glass needle using a high-temperature epoxy resin. This single-crystal was used for the collection of the X-ray data sets at room temperature, 245 °C, and during the temperature-dependent intensity measurements of selected reflections between −163 and 245 °C.

X-ray intensities were measured on a CAD4 Enraf-Nonius diffractometer using graphite-monochromatized Mo$K\alpha$ radiation. Data up to $\theta = 40°$ were collected in ⅜ of a sphere in reciprocal space (always including one hkl and $-hkl$ set) in the 1.5° ω-scan mode. Additional experimental conditions are summarized in Table 1. During the high-temperature measurements the crystal was heated by a regulated (±5 °C) hot-air blower. In the low-temperature experiments a conventional liquid-nitrogen cooling device with an accuracy of ±2 °C was used. The exact temperatures were calibrated by a specially designed goniometer head with a thermocouple mounted at the crystal position.

An empirical absorption correction was applied using the ψ-scan technique. Data reduction, including background and Lorentz-polarization corrections, was performed with the SDP program (Enraf-Nonius 1983). The program SHELXTL (Siemens 1990) was used for the refinement of the $Cmcm$ structure. Because twinning parallel to (100) was found in the $P2_1cn$ structure, the program SHELXL-93 (Sheldrick 1993) was applied, which allows for refinement of twinning contributions on the basis of F^2. Additional twinning and disorder in the $P2_1cn$ structure was modeled by symmetric constraints of various atomic positions. Neutral atom scattering factors were used in all refinements. H atoms were located on difference-Fourier maps and subsequently refined using a constraint of O-H = 0.80(2) Å as adopted from the results of the lawsonite refinements (Libowitzky and Armbruster 1995). In all refinements structure factors F or F^2 were weighted $1/\sigma^2$.

To obtain additional information about the behavior of the phase transitions, unit-cell parameters were refined from 14 reflections (18° < θ < 30°) at 15 temperatures between 22 and 245 °C. The exact transition temperatures were determined by intensity vs. temperature measurements of the strongest C-centering forbidden reflection 017 and by the 406 reflection, which proved to be most sensitive for the $P2_1cn$ transition. In addition, ω profiles of different, strong reflections were recorded at temperatures between −163 and 245 °C to investigate a monoclinic lattice distortion at temperatures below ~100 °C.

Unfortunately, an optical investigation of the phase transitions and of the twin-domain evolution was not feasible because of the intense brown color and the high refractive index (>1.82) of hennomartinite. In all orthorhombic twin or disorder models considered for hennomartinite, the orientation of the optical indicatrix remains unchanged.

RESULTS

Initial investigation of the hennomartinite crystal on the single-crystal diffractometer proved the existence of several C-centering forbidden reflections (hkl, with $h + k = 2n + 1$), thus violating a C-centered cell (Armbruster et al. 1992). C-centering forbidden reflections can be recorded only for high-quality crystals because the intensity of the $h + k = 2n + 1$ reflections is very weak. The strongest of these reflections, 017, with $I = 20\sigma_I$, is also the strongest C-centering forbidden reflection ($I = 40\sigma_I$) in the primitive structures of lawsonite at low temperatures (Libowitzky and Armbruster 1995). The room temperature hennomartinite data set was in agreement with the general reflection conditions and refined as a twin parallel to (100) in space group $P2_1cn$ with a final $R = 2.0\%$. Test refinements in space groups with higher symmetry ($Pmcn$, $Pmcm$) and an untwinned refinement in $P2_1cn$ always resulted in unsatisfactory R values or high residual electron densities and thus did not allow the determination of the H positions. The 017 reflection was also used to monitor the stability field of the primitive
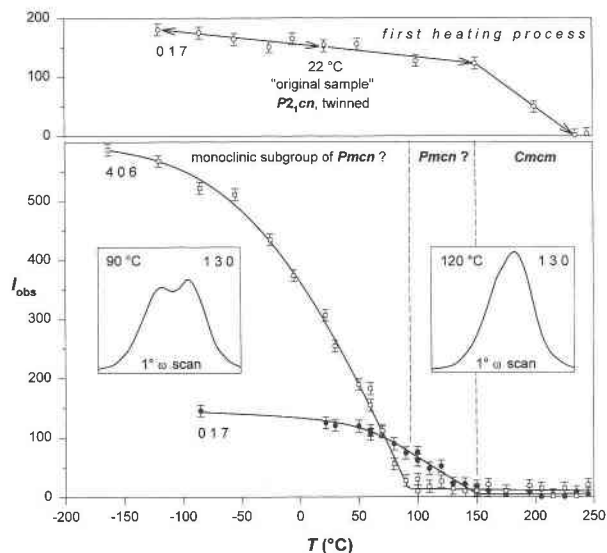
FIGURE 1. Intensity (arbitrary units) vs. temperature for the 406 and 017 X-ray reflections, which were used to monitor the reversible phase transitions at 95(5) and 150(5) °C in hennomartinite. The upper window of the graph shows the irrecoverable development of the 017 reflection disappearing only at ~235 °C during the first heating process. The two small square insets give an example of ω scans of an unsplit $hk0$ reflection (130) above ~100 °C and the split equivalents below 100 °C.

phase during a cooling and first heating experiment. In the temperature range −163–150 °C, the 017 intensity remained almost constant. At 200 °C it dropped to only $6\sigma_I$ above background, and at 235 °C it disappeared (Fig. 1, upper plot). Thus, a temperature of 245 °C was chosen to measure a C-centered data set of hennomartinite. In accordance with the general reflection conditions it was refined in space group $Cmcm$ to a final $R = 2.3\%$.

For a better understanding of the structures and phase transition, the authors prefer to begin with the description of the 245 °C structure of hennomartinite, which is isotypic with the room temperature $Cmcm$ structure of lawsonite (Libowitzky and Armbruster 1995).

Hennomartinite, *Cmcm* structure

The final atomic positional parameters of hennomartinite at 245 °C in space group $Cmcm$ are summarized in Table 2. Anisotropic displacement factors are presented in Table 3, and a list of observed and calculated structure factors is given in Table 4.[1] A projection of the structure parallel to [100] is drawn in Figure 2. The structure consists of rods of edge-sharing, Jahn-Teller–distorted MnO_6 octahedra that run parallel to [100] and are interconnected by Si_2O_7 groups. The remaining interstices of the framework are occupied by Sr, an H_2O molecule (O5, Hw

---

[1] A copy of Table 4 may be ordered as Document AM–96–607 from the Business Office, Mineralogical Society of America, 1015 Eighteenth Street NW, Suite 601, Washington, DC 20036, U.S.A. Please remit $5.00 in advance for the microfiche.

TABLE 2. Atomic positional parameters for hennomartinite, $Cmcm$, at 245 °C

Atom	x	y	z	B_{eq} (Å²)
Sr	0	0.31258(4)	¼	1.556(5)
Mn	¼	¼	0	0.885(4)
Si	0	0.96991(7)	0.13224(4)	0.769(8)
O1	0	0.0198(3)	¼	1.51(4)
O2	0.2851(2)	0.3723(1)	0.11492(9)	1.28(2)
O3	0	0.1275(2)	0.0768(1)	1.26(2)
O4	0	0.6340(2)	0.0424(2)	1.38(2)
O5	0.029(4)*	0.6068(5)	¼	3.1(3)
Hw	0	0.637(6)	0.198(2)	4.74**
Hh	0	0.552(2)	0.046(4)	7.11**

* Split-atom position.
** Fixed isotropically.

× 2), and an OH site (O4, Hh), which has twice the multiplicity of O5 (two OH groups per formula unit). Selected interatomic distances and angles are given in Table 5.

Sr is coordinated by eight O atoms at distances between 2.60 and 2.87 Å. The Jahn-Teller distortion of the MnO_6 polyhedron is characterized by four short [1.91 Å (× 2) and 1.97 Å (× 2)] and two long (2.18 Å) Mn-O bonds. The octahedral angles are almost regular, yielding values close to 90°. The Si-O distances range from 1.61 to 1.65 Å. The Si-O-Si' angle of the Si_2O_7 group is 148°, which is wider than that in lawsonite (137°).

There are two appropriate ways to describe the position of the H_2O molecule: (1) O5 at a special position $(0,y,\frac{1}{4})$ with site symmetry $m2m$. In this case U_{11} exhibits a value of 0.07 Å², whereas U_{22} and U_{33} are 0.04 and 0.03 Å², respectively. (2) O5 at a split atom position with $x = 0.03$ (slight deviation of ±0.18 Å from the special position), which consequently lowers U_{11} to 0.05 Å². Model (1) represents a dynamically (time-averaged) and model (2) a statically (space-averaged) disordered H_2O displacement. Although the latter model may be more reasonable (as is assumed in Tables 2 and 3), both cases refined to identical R values. Moreover, a test refinement in space group $C2cm$, using a 1:1 twin model parallel to (100) instead of the split O5 position, resulted in a comparably low R value and thus cannot be excluded (as discussed later).

The constrained O5-Hw distances converged to 0.77(3) Å. These distances seem to be short compared with those in a free H_2O molecule (0.98 Å). However, they are in quite good agreement with O-H distances from other X-ray investigations, and they are probably caused by the delocalized H electron (Lager et al. 1987). The H-O-H angle [130(6)°] is rather large compared with the angle in a free H_2O molecule (104.5°). This is probably because of the high uncertainty of the H positions and the strong libration of the H_2O molecule. In addition, there are two hydrogen bonds to O4 atoms (2.09 Å).

The H atoms of the OH groups are bonded to O4 at a distance of 0.75(2) Å. As in lawsonite the O4-Hh vectors are almost parallel to the b axis. Additional O $\cdots$ H distances are as far as 2.06 Å, thus forming a hydrogen bond with O4'.

It must be concluded that the $Cmcm$ structure of hen-

TABLE 3. Anisotropic displacement parameters for hennomartinite, *Cmcm*, at 245 °C

Atom	U_{11}	U_{22}	U_{33}	U_{12}	U_{13}	U_{23}
Sr	0.0227(2)	0.0220(2)	0.0144(1)	0	0	0
Mn	0.0109(1)	0.0116(1)	0.0112(1)	−0.0004(1)	0.0001(1)	−0.0027(1)
Si	0.0120(2)	0.0090(2)	0.0082(2)	0	0	0
O1	0.028(1)	0.022(1)	0.0077(8)	0	0	0
O2	0.0144(5)	0.0178(5)	0.0164(5)	−0.0039(4)	0.0018(4)	−0.0055(4)
O3	0.0216(8)	0.0115(6)	0.0148(7)	0	0	0.0038(6)
O4	0.0181(8)	0.0127(6)	0.0216(8)	0	0	0.0032(6)
O5	0.05(1)	0.037(2)	0.025(2)	0	0	0

nomartinite at 245 °C (Fig. 2) and that of lawsonite at temperatures >0 °C (Fig. 2 in Libowitzky and Armbruster 1995) are extremely similar.

Hennomartinite, $P2_1cn$ structure

The primitive X-ray single-crystal data set collected at room temperature (22 °C) was refined in space group $P2_1cn$ to a final $R = 2.0\%$. However, only the introduction of a twin model led to the location of the H atoms in the final refinement. Because Sr and Mn show appreciable anomalous scattering effects (the absorption edge of Sr is very close to the Mo$K\alpha$ emission line), the hkl vs. $-hkl$ Friedel pairs are no longer equivalent in an acentric space group. Thus, one must refine the correct crystal orientation and the correct portions of the two, oppositely oriented, polar twin domains. As indicated by space group

FIGURE 2. The *Cmcm* structure of hennomartinite at 245 °C projected along [100]. The edge-sharing, Jahn-Teller–distorted MnO$_6$ octahedra form rods parallel to [100], which are interconnected by Si$_2$O$_7$ groups. The interstices of the framework are occupied by Sr atoms (large spheres) and H$_2$O molecules (O5 = medium spheres), and by the H atoms (small spheres) of the OH groups. Dotted lines represent O $\cdots$ H bonds between 2.0 and 2.1 Å.

$P2_1cn$ (polar a axis), the twin plane is (100). The twin refinement led to final twin contributions of 43 and 57%, respectively. In addition, ~7% disorder (x,y,z; $-x,y,z$) was considered. Moreover, the final difference-Fourier summations showed that the H atoms statistically occupy split atom positions with x,y,z (L) and $x,y,0.5 - z$ (R). The importance of these twin and disorder relations is discussed later.

The final atomic positional parameters of the 22 °C $P2_1cn$ hennomartinite structure are given in Table 6, anisotropic displacement factors are presented in Table 7, and structure factors are listed in Table 4. Standard deviations of positional parameters in the $P2_1cn$ structure are considerably larger than in the *Cmcm* structure at high temperature. This is caused by correlation problems in the $P2_1cn$ refinement because the octahedral-tetrahedral framework possesses nearly *Cmcm* symmetry. A projection of the structure parallel to [100] is shown in Figure 3.

Compared with the 245 °C *Cmcm* structure of hennomartinite, the Sr, Mn, Si, and O atoms show maximum shifts of 0.16 Å (usually parallel to [100] representing the polar direction). Thus, as in lawsonite, the framework of the structure behaves quite rigidly, and the principal changes of the structure are related to shifts of the H atoms and the effects of these shifts on neighboring atoms. In comparison with the 245 °C refinement, the B values decreased by about one-half, which is in good agreement with the ratio observed in the lawsonite refinements (Libowitzky and Armbruster 1995). The coordination polyhedra around Sr, Mn, and Si are almost the same as in the 245 °C *Cmcm* hennomartinite structure, except that they are slightly more distorted than their counterparts in *Cmcm* (a consequence of the reduced symmetry of space group $P2_1cn$). Even the Jahn-Teller distortion of the MnO$_6$ octahedra is similar in both structures (Table 5).

Although the H atoms are on special positions (mirror plane m- - at $x = 0$) and are symmetrically related (mirror plane - -m at $z = 0.25$) in the *Cmcm* structure, in the $P2_1cn$ structure the H positions split by rotation within the (100) plane into an Hw-Hw1 and an Hh-Hh1 site. Moreover, one H atom (Hw) of the H$_2$O molecule shifts considerably below m- - ($x = -0.15$; −0.94 Å). The other one (Hw1) remains close to that plane ($x = -0.02$; −0.12 Å). Because of the decrease of the x coordinate of the Hw atom, the O atom of the H$_2$O molecule (O5) also shifts
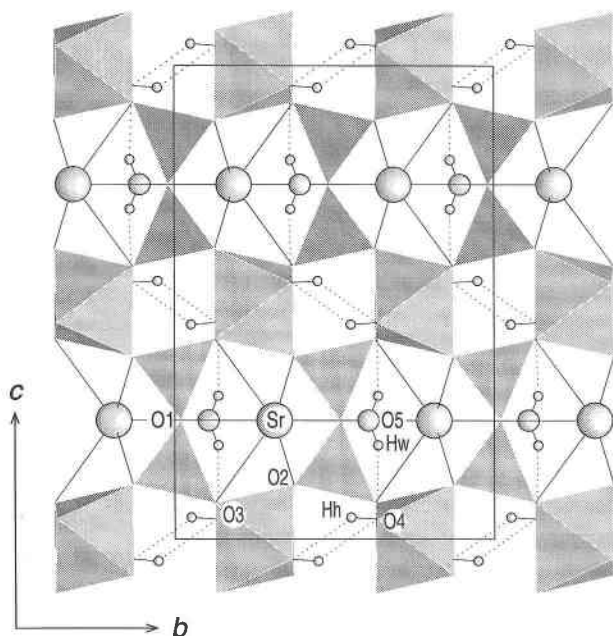
TABLE 5. Selected interatomic distances (Å) and angles in hennomartinite at 245 °C (*Cmcm*) and 22 °C (*P2₁cn*)

245 °C, *Cmcm*		22 °C, *P2₁cn*			
Sr-O2 × 4	2.601(1)	Sr-O2	2.547(9)	Sr-O22	2.643(8)
Sr-O1	2.654(3)	Sr-O21	2.566(9)	Sr-O5	2.693(4)
Sr-O5	2.673(5)	Sr-O23	2.620(8)	Sr-O31	2.835(7)
Sr-O3 × 2	2.869(2)	Sr-O1	2.641(3)	Sr-O3	2.897(7)
Mn-O2 × 2	1.913(1)	Mn-O2	1.908(8)	Mn1-O21	1.895(8)
Mn-O4 × 2	1.968(1)	Mn-O23	1.931(7)	Mn1-O22	1.908(7)
Mn-O3 × 2	2.178(1)	Mn-O41	1.973(9)	Mn1-O4	1.948(9)
		Mn-O41′	1.994(9)	Mn1-O4′	1.986(9)
		Mn-O3	2.122(11)	Mn1-O31	2.143(10)
		Mn-O3′	2.199(10)	Mn1-O31′	2.220(11)
Si-O3	1.611(2)	Si-O3	1.604(9)	Si1-O2	1.615(12)
Si-O2 × 2	1.626(1)	Si-O1	1.621(12)	Si1-O31	1.628(9)
Si-O1	1.645(1)	Si-O22	1.628(11)	Si1-O23	1.633(10)
		Si-O21	1.629(9)	Si1-O1	1.668(12)
Si-O1-Si	148.1(2)	Si-O1-Si1	146.8(3)		
Hw-O5	0.77(3)	HwL-O5	0.80(5)	HwR-O5	0.79(4)
Hw···O4	2.09(3)	Hw1L-O5	0.77(4)	Hw1R-O5	0.84(4)
		Hw1L···O4	1.99(4)	Hw1R···O4	2.12(4)
Hw-O5-Hw	130(6)	HwL-O5-Hw1L	97(16)	HwR-O5-Hw1R	92(16)
Hh-O4	0.75(2)	HhL-O41	0.80(7)	HhR-O4	0.79(8)
		HhL···O5	2.28(6)	HhR···O5	2.22(6)
Hh···O4′	2.06(3)	Hh1L-O4	0.83(6)	Hh1R-O41	0.76(7)
		Hh1L···O41	1.86(7)	Hh1R···O4	1.99(7)

Note: Minimum O-H distances were constrained to 0.80(2) Å during refinement. Estimated standard deviation of the last decimal is in parentheses.

in the x direction below the zero level ($x = -0.025$; -0.16 Å). Compared with the *Cmcm* structure, some hydrogen bonds are strengthened (Hw1L ⋯ O4 = 1.99 Å; Hw1R ⋯ O4 = 2.12 Å), whereas others are weakened (Hw ⋯ O1 = 2.50 Å). The differences between L and R H atoms are probably caused by a simple disorder model (involving only the H atoms).

The H atom (Hh) of one hydroxide group also shifts considerably below the zero level ($x = -0.09$; -0.56 Å). The second H atom (Hh1) remains close to the zero plane ($x = 0.03$; 0.19 Å), enhancing the former *Cmcm* hydrogen bond (Hh ⋯ O4′ = 2.06 Å) to 1.86 Å (Hh1L ⋯ O41) and 1.99 Å (Hh1R ⋯ O4). The Hh atoms exhibit additional long hydrogen bonds with 2.28 Å (HhL ⋯ O5) and 2.22 Å (HhR ⋯ O5).

In the 110 K $P2_1cn$ structure of lawsonite (Libowitzky and Armbruster 1995) Hw shifts below and Hh shifts above the zero level (opposite to hennomartinite), but the general tendency to enhance the hydrogen bond system at low temperatures is common to both minerals. The shift of the H atoms is probably caused by reduced thermal libration, which constrained the H_2O molecules and OH groups to occupy highly symmetric positions in the interstitial "cavities" of the 245 °C *Cmcm* structure. When thermal vibration is reduced, the cavities of the structure become oversized, and the OH groups and H_2O molecules are attached by hydrogen bonds to the walls of the cavities.

It is also highly plausible that the rotation of the H_2O and OH groups does not occur in the same way within the whole crystal. It seems more probable that there is extensive twinning, ranging from local disorder to extensive twin-domain formation, which is confirmed by the $P2_1cn$ twin refinement.

Monitoring of distinct reflections

As mentioned above, the C-centering forbidden reflection 017 disappeared during the first heating process between 200 and 235 °C. After collection of the 245 °C X-ray data the crystal was slowly cooled down. During this process the intensity of the 017 reflection was monitored to confirm the reappearance of a primitive struc-

TABLE 6. Atomic positional parameters for hennomartinite, $P2_1cn$, at 22 °C

Atom	x	y	z	B_{eq} (Å²)
Sr	0.01703	0.31155(4)	0.2517(1)	0.676(7)
Mn	0.2454(5)	0.2566(2)	−0.0051(1)	0.389(4)
Mn1	0.2482(5)	0.2508(2)	0.5023(2)	0.389(4)
Si	−0.001(1)	0.9715(5)	0.1315(2)	0.415(8)
Si1	−0.004(1)	0.9670(5)	0.3667(2)	0.415(8)
O1	−0.0179(8)	0.0202(3)	0.2477(9)	0.69(4)
O2	0.282(2)	0.372(1)	0.1130(5)	0.60(2)
O21	0.280(2)	0.379(1)	0.3915(5)	0.60(2)
O22	−0.287(1)	−0.3718(9)	−0.1171(4)	0.60(2)
O23	−0.294(1)	−0.3594(9)	−0.3752(5)	0.60(2)
O3	0.001(2)	0.128(1)	0.0746(5)	0.63(2)
O31	0.011(2)	0.127(1)	0.4227(4)	0.63(2)
O4	−0.001(1)	0.6368(7)	0.0462(4)	0.62(3)
O41	−0.017(2)	0.6269(7)	0.4631(5)	0.62(3)
O5	−0.025(1)	0.6082(4)	0.2475(7)	2.04(8)
HwL	−0.148(5)	0.626(9)	0.26(1)	3.95*
HwR	−0.148(5)	0.626(9)	0.24(1)	3.95*
Hw1L	−0.02(2)	0.642(8)	0.195(3)	3.95*
Hw1R	−0.02(2)	0.642(8)	0.305(3)	3.95*
HhL	−0.09(1)	0.61(1)	0.415(4)	6.32*
HhR	−0.09(1)	0.61(1)	0.085(4)	6.32*
Hh1L	0.03(2)	0.551(6)	0.030(8)	6.32*
Hh1R	0.03(2)	0.551(6)	0.470(8)	6.32*

Note: L and R mark the respective split H positions (x, y, z; x, y, 0.5 − z). The twinned domain structure was refined with fractions of 7% disorder (−x, y, z) and 43% twin fraction (−x, y, z).
* Fixed isotropically.

TABLE 7. Anisotropic displacement parameters for hennomartinite, $P2_1cn$, at 22 °C

Atom	U_{11}	U_{22}	U_{33}	U_{12}	U_{13}	U_{23}
Sr	0.0080(3)	0.0100(1)	0.0077(1)	−0.0009(2)	0.0029(7)	0.0003(6)
Mn	0.0056(1)	0.0046(1)	0.0047(1)	0.0003(2)	−0.0021(8)	0.0016(5)
Mn1	0.0056(1)	0.0046(1)	0.0047(1)	0.0003(2)	−0.0021(8)	0.0016(5)
Si	0.0063(2)	0.0044(3)	0.0051(2)	0.0000(3)	−0.001(1)	0.001(1)
Si1	0.0063(2)	0.0044(3)	0.0051(2)	0.0000(3)	−0.001(1)	0.001(1)
O1	0.012(1)	0.0095(9)	0.005(1)	−0.001(1)	−0.005(4)	−0.001(3)
O2	0.0088(5)	0.0073(7)	0.0065(6)	−0.0016(5)	−0.002(2)	−0.002(2)
O21	0.0088(5)	0.0073(7)	0.0065(6)	−0.0016(5)	−0.002(2)	−0.002(2)
O22	0.0088(5)	0.0073(7)	0.0065(6)	−0.0016(5)	−0.002(2)	−0.002(2)
O23	0.0088(5)	0.0073(7)	0.0065(6)	−0.0016(5)	−0.002(2)	−0.002(2)
O3	0.009(1)	0.0065(5)	0.0085(6)	0.0001(9)	0.001(3)	−0.001(3)
O31	0.009(1)	0.0065(5)	0.0085(6)	0.0001(9)	0.001(3)	−0.001(3)
O4	0.008(1)	0.0078(8)	0.0081(9)	−0.0007(9)	0.001(2)	−0.001(1)
O41	0.008(1)	0.0078(8)	0.0081(9)	−0.0007(9)	0.001(2)	−0.001(1)
O5	0.037(3)	0.021(1)	0.019(2)	−0.006(2)	−0.019(5)	0.000(4)

ture of hennomartinite. However, the 017 reflection did not appear (as might be expected from the first heating process) at ~200 °C. At 160 °C the 017 intensity was still below the $1\sigma_I$ limit, and at 150 °C it increased slowly with values between 1 and $2\sigma_I$ (Fig. 1, main plot). At 100 °C the 017 reflection reached an intensity of only $7\sigma_I$.

The phase transitions in lawsonite, $P2_1cn$-$Pmcn$-$Cmcm$ (Libowitzky and Armbruster 1995), also suggest the presence of an intermediate phase between the $P2_1cn$ and $Cmcm$ hennomartinite structures. By analogy to lawsonite, $Pmcn$ may also be the intermediate space group in hennomartinite. This space group is a primitive subgroup of $Cmcm$ and a centrosymmetric supergroup of $P2_1cn$. To find a reflection for monitoring the assumed transition

FIGURE 3. The $P2_1cn$ structure of hennomartinite at 22 °C projected along [100]. Only one untwinned atom set and only the L H atom positions are shown. Dotted lines represent O···H bonds between 1.8 and 2.3 Å. Symbols as in Figure 2.

$Pmcm$-$P2_1cn$, the 22 °C data set was refined in the (inappropriate) higher space group $Pmcn$. The reflections that showed the most severe deviations between F_{obs} and F_{calc} (with F_{calc} close to zero) were selected and checked at different temperatures. The 406 reflection was the most significant of these and was monitored during the cooling process described above. As shown in Figure 1 (main plot), the intensity of the 406 reflection increased dramatically below 95(5) °C. Thus, the 150 °C transition represents the $Cmcm$-$Pmcn$ boundary, and, as a consequence, the proposed $Pmcn$ hennomartinite phase covers the gap between 95 and 150 °C. In lawsonite (Libowitzky and Armbruster 1995), this phase occupied an even broader field between 155 and 273 K (−118–0 °C). Considering the larger cations (Sr, Mn) and the larger unit-cell parameters of hennomartinite (in comparison with lawsonite), the phase transitions at higher temperatures are quite reasonable.

However, the space group $Pmcn$ is only suggested because the measurement and successful refinement of a primitive data set (I_{017} with only $6\sigma_I$) did not seem promising. Even if details of the $Pmcn$ hennomartinite structure cannot be presented, the basic principles can be inferred from the lawsonite $Pmcn$ structure. The framework is similarly almost rigid, and only the positions of the H atoms change. Representing a transition structure between $Cmcm$ and $P2_1cn$, the H atoms occupy positions between those of $Cmcm$ and $P2_1cn$. As described for the $P2_1cn$ structure, they rotate within the (100) plane (with increasingly distinct hydrogen bonds), thus splitting the symmetrically related $Cmcm$ Hw and Hh positions into Hw-Hw1 and Hh-Hh1 (loss of the --m mirror plane at $z = 0.25$). In contrast to the $P2_1cn$ phase, the Hw and Hh atoms do not shift below the x zero plane. Nevertheless, similar to the $Cmcm$ hennomartinite structure, a 1:1 twin parallel to (100) composed of two polar twin domains cannot be excluded. Hence, speaking of an average $Pmcn$ structure seems to be more correct.

During the subsequent heating and cooling cycles an unexpected increase in the widths of selected peaks (used for repeated refinement of the orientation matrix at different temperatures) with decreasing temperature was ob-
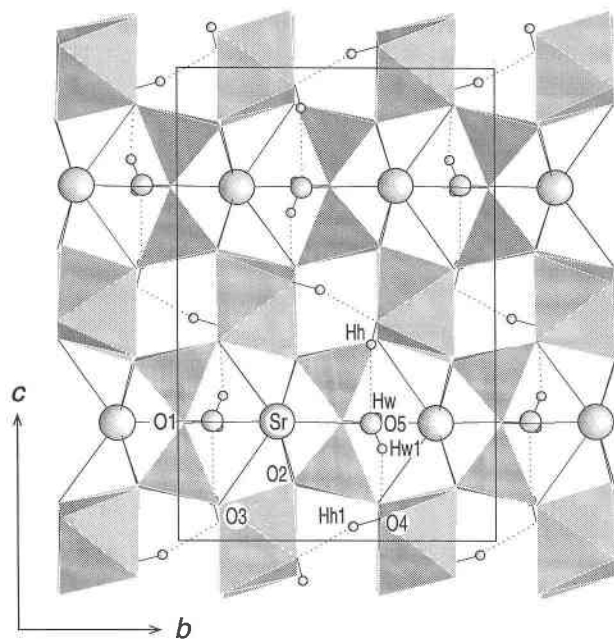
served. A closer look revealed a splitting or broadening (or both) of $hk0$ reflections in ω scans, whereas the $00l$ reflections remained sharp and unsplit over the whole temperature range. One of the most intense split peaks (130) was checked in detail by individual ω scans between -163 and $+200$ °C. As shown in the two small insets of Figure 1, the peak broadening starts near 120(5) °C and develops into a split peak at 90(5) °C. There is strong evidence that the peak splitting is intimately associated with the assumed $Pmcn$-$P2_1cn$ phase transition at 95(5) °C. An accurate peak decomposition of the ω profiles vs. intensity (using the program PeakFit, Jandel Scientific) into two Voigt-shaped curves showed that the peak area of the split and unsplit peaks (at low and elevated temperatures) remained constant, whereas the amount of angular splitting increased from almost 0° at 120 °C to 0.25° at 90 °C and finally to 0.33° ω at -163 °C.

The splitting in ω must be interpreted as a symmetry degeneracy from the orthorhombic to the monoclinic system, thus producing a twinned crystal with slightly tilted domains. Because $00l$ reflections are not affected by the splitting, c is the unique axis. The resulting phase may represent a monoclinic subgroup of space group $P2_1cn$ or $Pmcn$. A definite answer cannot be given because the split peaks do not allow accurate X-ray single-crystal data collection or space group determination. It must be stressed that during the data collection of the original 22 °C $P2_1cn$ phase (performed prior to the heating and cooling cycles) all peaks were sharp and unsplit. These apparently contradictory observations will be discussed below.

Repeated heating and cooling cycles led to the same results concerning the transition temperatures, the intensity of monitored peaks, and the amount of splitting below 100 °C. Thus, the process is reversible.

Additional experiments, such as annealing the crystal for 16 h at 80 °C and quenching the crystal from 200 °C to room temperature, did not show significant change in the transition behavior of hennomartinite or in the split peak profiles. These experiments confirm that the crucial structural evolution occurred after the first heating process during annealing at elevated temperature. The initial state of the crystal could not be recovered.

Changes in unit-cell parameters

The behavior of the unit-cell parameters (a, b, c) and the cell volume (V) vs. temperature (22–245 °C) is plotted in Figure 4. Starting points are always the values at 22 °C, at which temperature the initial $P2_1cn$ hennomartinite data set was collected. The most significant observation is the impressive decrease of a and V (b and c only to a minor extent), which occurred at constant temperature (for ~4 d) during the measurement of the 245 °C $Cmcm$ hennomartinite data set. Even if this decrease amounts to only 0.3% in a and V, it is highly significant above a 3σ level. The path of the subsequent cooling and heating cycles is parallel to the first heating process but shifted by -0.3%; it is identical (within estimated standard deviations) for additional cooling and heating cy-

cles. These experiments clearly confirm that the crucial structural evolution occurred during the 245 °C data collection.

A possible release of H_2O cannot explain the decrease of a and V because the structure refinement at 245 °C shows that the O5 position (water molecule) remained completely occupied. Moreover, a comparative thermogravimetric analysis (TGA) of lawsonite showed that loss of water takes place above 550 °C. (A TGA of hennomartinite was impossible because of the extremely small amount of material.) In addition, the idea of a change of the Mn^{3+} valence must be rejected because the Jahn-Teller distortion is always present and a change of Mn valence is not expected for charge neutrality and bond strength reasons. This was also confirmed by a bond-valence calculation, which resulted in equal values (within estimated standard deviation) for the $Cmcm$ and $P2_1cn$ structures.

In contrast to lawsonite (Libowitzky and Armbruster 1995), a nonlinear change in unit-cell parameters at the phase boundaries was not observed. The large errors of the unit-cell parameters below 100 °C are caused by the above mentioned peak splitting. The unusual decrease of unit-cell parameters during the annealing at 245 °C may be related to a twin-domain evolution in hennomartinite, as discussed in the following section.

DISCUSSION

The present investigation clearly demonstrates that hennomartinite and lawsonite are isostructural at the respective temperatures, and that the phase transitions are of the same type with respect to the principal mechanisms involved. The reader is referred to the paper on lawsonite (Libowitzky and Armbruster 1995), where the sub- and supergroup relations are elucidated. Recent papers on titanite (Bismayer et al. 1992) and quartz (Kihara 1990) give additional information about reversible, displacive phase transitions.

The most striking difference between the lawsonite and the hennomartinite transitions is the existence of an additional monoclinic distortion at low temperatures and complicated disorder and twinning behavior.

To elucidate the difference between disorder and twinning and to demonstrate their influence on X-ray intensities one must consider the following: (1) Both disorder and twinning produce a second set of atoms, B, which can be derived from the original atom set A by a geometric (twin) transformation. In the case of hennomartinite the following transformations occur: x,y,z; $-x,y,z$ disorder + twin, and x,y,z; and $x,y,0.5 - z$ disorder. (2) The difference between disorder and domain or twin formation is given by the size of extension of the A and B set. If this size is smaller than the size of the diffracting unit it appears as disorder. If it exceeds the size of the diffracting unit a domain or twin is observed. (3) The amount of twinning, disorder, or both can, in principle, be extracted (and refined) from the X-ray intensities (Dunitz 1979). (4) In the case of twinning we find $I \approx$
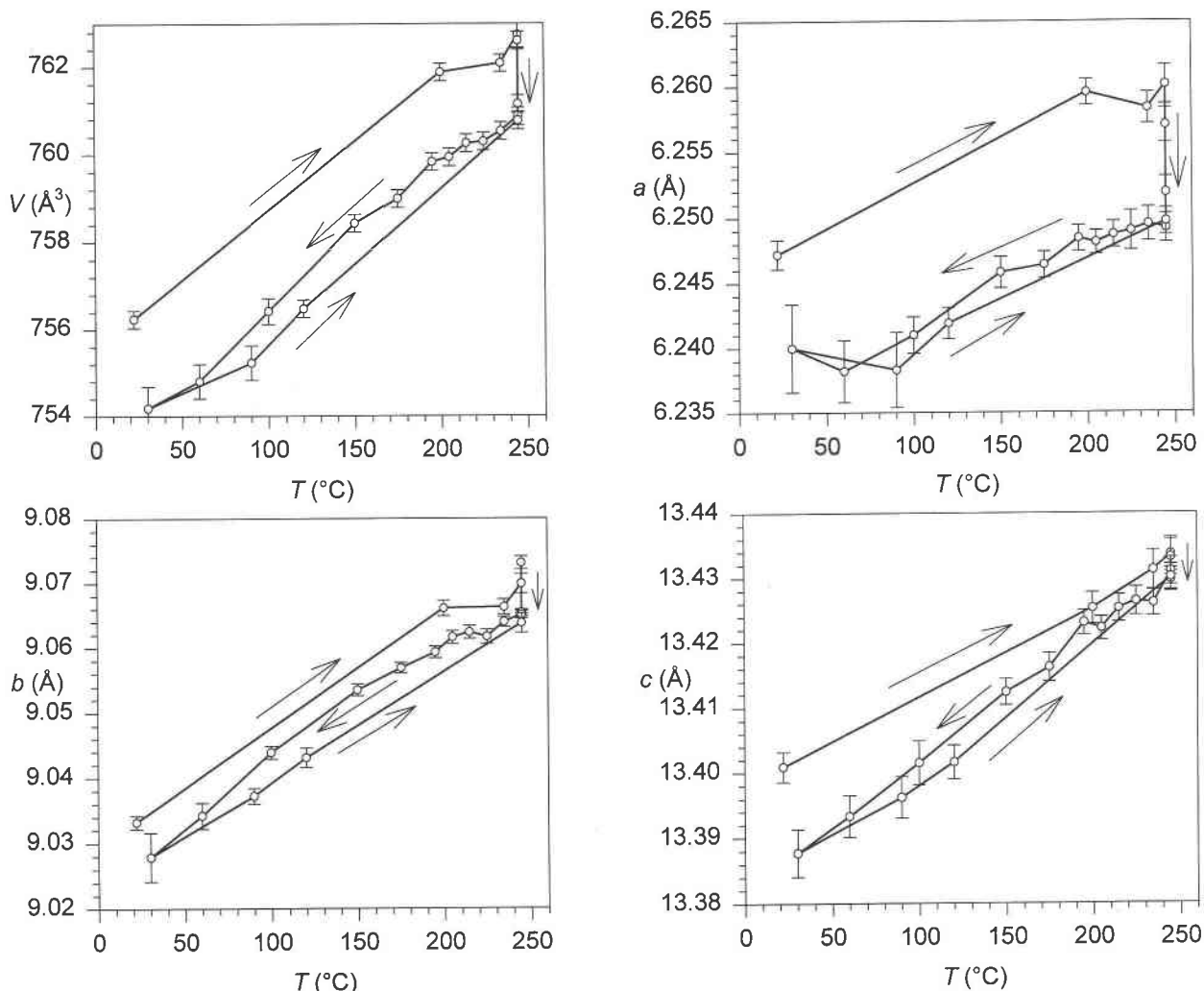
FIGURE 4. Plot of unit-cell parameters (a, b, and c) and V of lawsonite vs. temperature. The heating and cooling path is indicated by arrows starting at 22 °C.

$F_A^2 + F_B^2$, where F is the structure factor of the atom sets A and B. Thus, the twin law should be applied directly to F^2. (5) In the case of disorder we find $I \approx (F_A + F_B)^2 = F_A^2 + F_B^2 + 2F_A F_B$; thus disorder is modeled on the basis of atomic coordinates.

Twinning is detectable on a broad scale in the hennomartinite $P2_1cn$ refinement, whereas in lawsonite (Libowitzky and Armbruster 1995) no twinning was found. However, as shown by a proton NMR study (S.P. Gabuda and S.G. Kozlova, personal communication), dynamic (time-averaged) disorder must be considered in the $Cmcm$ lawsonite phase.

In hennomartinite the Sr atom shows extremely strong anomalous scattering effects for Mo$K\alpha$ radiation. Consequently, the Friedel equivalents of reflections may yield different intensities. Hence, refinement of the absolute crystal orientation and the amount of twinning can be performed with low estimated standard deviations, and, of course, the twin model also has a strong influence on the final R values of a $P2_1cn$ refinement. The resulting

values of a 43:57% twinning parallel to (100) plus approximately 7% disorder with coordinates $-x,y,z$ provides good evidence for the existence of fine twin domains, even if the actual size of the domains cannot be determined. In addition, the H atoms were found to be disordered with x,y,z and $x,y,0.5 - z$ coordinates. An additional twin refinement was not performed because an - -m twin mirror plane yields the same intensity ratios between Friedel-related reflections as the untwinned $P2_1cn$ model.

The description of the $P2_1cn$ hennomartinite structure that was initially determined at 22 °C represents a unique, irrecoverable starting point in the evolution of a rather complicated twin-disorder pathway of hennomartinite during subsequent heating and cooling experiments (Figs. 1 and 4): (1) The P (primitive) to C-centered transition occurs above 200 °C during the first heating process. (2) With the temperature kept constant for ~4 d at 245 °C, the a unit-cell parameter decreases by 0.3% and remains at this new value during subsequent cooling and heating

cycles. (3) The high U_{11} value of O5 justifies a refinement of the 245 °C *Cmcm* structure with a split $(x, y, \frac{1}{4}; -x, y, \frac{1}{4})$ O5-atom position [statically (space-averaged) disordered model]. A 1:1 twin model parallel to (100) in space group *C2cm* cannot be excluded. (4) After cooling from 245 °C, the C-P transition (leading to the assumed space group *Pmcn*) is found at 150 °C. (5) Around 95 °C, a further transition leads (as indicated by split peaks) to some monoclinic subgroup ($\gamma \neq 90°$) of the primitive orthorhombic space group. (6) Subsequent heating and cooling cycles yield identical transition temperatures and unit-cell parameters, indicating the reversibility of the process. (7) Quenching from 200 °C and annealing at 80 °C yield identical results in subsequent cycles.

The most probable evolution path of disorder and twinning in hennomartinite is drawn in Figure 5. At 22 °C the $P2_1cn$ structure of hennomartinite consists of small twin domains (probably just above the size of the diffracting unit) with orientations corresponding to the positions x, y, z and $-x, y, z$. Additional 7% disorder (x, y, z and $-x, y, z$) may originate from the many twin-domain boundaries, or it may be caused by an additional contribution of domains that are smaller than the diffracting unit. Disorder of the H atoms with orientations x, y, z and $x, y, 0.5 - z$ complicates the situation. It is obvious that the H atoms have at least some effect on the z position of the O5 atoms. Because O5 shifts slightly from $z = 0.25$, it follows that, even though the disorder was refined with an approximate 1:1 ratio of the two orientations, the true ratio of disorder is somewhat different (with preference for set L). This is also confirmed by our observation of a primitive space group. If the ratio of disorder were exactly 1:1 it would result in a pseudo C-centered cell (Fig. 5). A monoclinic distortion (as observed in the low-temperature phase during subsequent heating and cooling cycles) is prohibited by the small twin domains, which constrain each other (for the benefit of a larger a unit-cell parameter) to an angle of $\gamma = 90°$.

During the first heating process the disorder of the H atoms disappears (in *Cmcm* the x, y, z and $x, y, 0.5 - z$ positions are symmetrically equivalent), thus leading to the 245 °C *Cmcm* structure of hennomartinite. However, the split O5 position suggests that the structure is composed of two oppositely oriented atom sets (at least visible in O5) with space group symmetry *C2cm* of the single unit. When collection of the 245 °C X-ray data set begins (large unit-cell parameter a) the twin domains are extremely small (equal or smaller than the diffracting unit). Hence, a description in *Cmcm* with a split atom position is almost the same as a description in two *C2cm* structures (x, y, z and $-x, y, z$) that are intergrown at the unit-cell level. During the data collection at 245 °C the twin domains begin to grow and the a unit-cell parameter decreases. Therefore, the correct description of the structure after data collection is a twin model with approximately equal fractions of the orientations given by the positions x, y, z and $-x, y, z$ in space group *C2cm*. Nevertheless, almost equal fractions of a *C2cm* twin cannot be proven because (as in the case of the centrosymmetric *Cmcm*
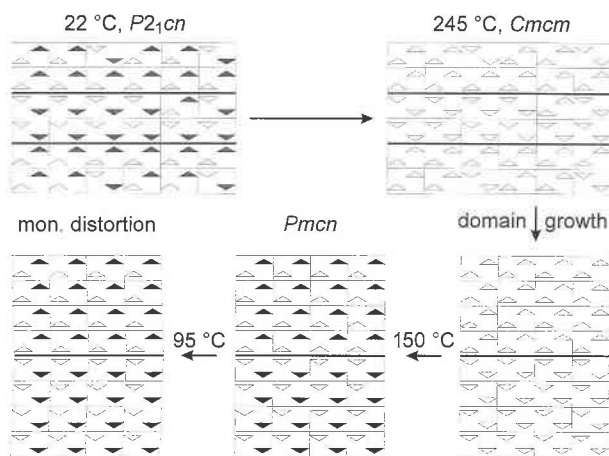

FIGURE 5. Sketch of the disorder–twin-domain evolution in hennomartinite. The rectangles represent the hennomartinite unit cells viewed along [001], thus showing the horizontal b axis and the vertical a axis. The triangles mark the polar aspect in the structure (e.g., the deviation of O5 from $x = 0$). Solid and open triangles indicate that structural elements (e.g., H_2O molecules) are rotated above and below, respectively, the plane of drawing preventing a C-centered space group. The bold lines mark domain boundaries.

structure) equal Friedel pairs result. This was also confirmed by a test twin refinement in space group *C2cm*, which yielded R values equivalent to those of the refinement in space group *Cmcm* (with and without the split O5 position).

If the crystal cools from 245 °C, the large twin domains remain unchanged. At 150 °C the C centering of the structure is disturbed by the different orientations of the H_2O and OH groups in the (100) plane. However, because of the large twin domains it is more appropriate to speak of an approximately 1:1 twinned crystal, with each of the domains showing $P2_1cn$ symmetry. It must also be assumed that the rotation of the H_2O and OH groups does not occur in an ordered fashion over the whole crystal, thus leading to additional disorder with orientations given by the positions x, y, z and $x, y, 0.5 - z$. The C-centering forbidden reflection 017, increasing very slowly below 150 °C, suggests that the ratio of disorder is close but not equal to 1:1. The different temperatures of the P-C transitions (above 200 °C during the first heating process, 150 °C in later experiments) can be explained by the varying domain size, which was small in the first heating cycle and large in subsequent cooling and heating cycles.

The strong enhancement of the 406 reflection below 95 °C indicates an additional hennomartinite phase. The splitting of reflections (except for 00*l*) below 100 °C suggests a monoclinic ($\gamma \neq 90°$) derivative of the primitive orthorhombic space groups. Because of the large twin domains (relative to the initially determined phase at 22 °C) the twin fractions are relaxed and undergo a monoclinic distortion adjusting for the polar deviation of the Sr, O1, O5, and H atoms. Because the O1-Sr-O5 vector is almost perpendicular to the c axis, and because the polar devi-

ations of the above mentioned atoms can be described by a rotation around the c axis, a monoclinic distortion of γ (with c as the unique axis) is in perfect agreement with this model.

As indicated by the subsequent heating and cooling cycles, which behave reversibly and thus repeatedly yield unchanged transition temperatures and lattice expansion and contraction, the large domain size remains almost unchanged between -163 and $245\ ^{\circ}$C. Hence, even annealing at $80\ ^{\circ}$C or quenching from $200\ ^{\circ}$C cannot produce any additional effects in the domain evolution.

The original $22\ ^{\circ}$C $P2_1cn$ hennomartinite phase in nature may be explained by growth at temperatures above $245\ ^{\circ}$C followed by rapid cooling, thus leading to an extremely fine domain size within the crystal. However, rapid cooling rates (close to quenching) seem to be incompatible with the small, hennomartinite-bearing veinlets crosscutting the sugilite matrix. On the other hand, fast metastable growth at low temperatures may be a more appropriate explanation for the formation of a small domain size in the original hennomartinite crystals. As indicated by the many hennomartinite crystals that were rejected during the preliminary selection procedure (owing to split peaks!, weak diffraction, etc.), many "initial states" seem to exist in the hennomartinite crystals. This observation also confirms a rapid metastable growth of hennomartinite.

ACKNOWLEDGMENTS

REFERENCES CITED

Armbruster, T., Oberhänsli, R., and Bermanec, V. (1992) Crystal structure of $SrMn_2[Si_2O_7](OH)_2 \cdot H_2O$, a new mineral of the lawsonite type. European Journal of Mineralogy, 4, 17–22.

Armbruster, T., Oberhänsli, R., Bermanec, V., and Dixon, R. (1993) Hennomartinite and kornite, two new Mn^{3+} rich silicates from the Wessels Mine, Kalahari, South Africa. Schweizerische Mineralogische und Petrographische Mitteilungen, 73, 349–355.

Baur, W.H. (1978) Crystal structure refinement of lawsonite. American Mineralogist, 63, 311–315.

Bismayer, U., Schmahl, W., Schmidt, C., and Groat, L.A. (1992) Linear birefringence and X-ray diffraction studies of the structural phase transition in titanite, $CaTiSiO_5$. Physics and Chemistry of Minerals, 19, 260–266.

Dunitz, J.D. (1979) X-ray analysis and the structure of organic molecules, 514 p. Cornell University Press, Ithaca, New York.

Enraf-Nonius (1983) Structure determination package (SDP). Enraf Nonius, Delft, the Netherlands.

Kihara, K. (1990) An X-ray study of the temperature dependence of the quartz structure. European Journal of Mineralogy, 2, 63–77.

Lager, G.A., Armbruster, T., and Faber, J. (1987) Neutron and X-ray diffraction study of hydrogarnet $Ca_3Al_2(O_4H_4)_3$. American Mineralogist, 72, 756–765.

Libowitzky, E., and Armbruster, T. (1995) Low-temperature phase transitions and the role of hydrogen bonds in lawsonite. American Mineralogist, 80, 1277–1285.

Sheldrick, G.M. (1993) SHELXL93: Program for crystal structure determination. University of Göttingen, Germany.

Siemens (1990) SHELXTL PC 4.1 (computer program). Siemens analytical X-ray instruments, Madison, Wisconsin.